JOURNAL OF MATERIALS SCIENCE **39** (2004) 5951–5957

Processing and characterization of ZrB_2-based ultra-high temperature monolithic and fibrous monolithic ceramics

W. G. FAHRENHOLTZ, G. E. HILMAS, A. L. CHAMBERLAIN, J. W. ZIMMERMANN
Department of Ceramic Engineering, University of Missouri-Rolla, Rolla, MO 65409, USA
E-mail: billf@umr.edu
Web: www.umr.edu/∼billf

Zirconium diboride (ZrB_2) based ultra-high temperature ceramics either unmodified or with SiC particulate additions of 10, 20, or 30 volume percent were prepared by conventional hot pressing. The ZrB_2-SiC compositions had improved four-point bend strength compared to the ZrB_2 prepared in our laboratory as well as other reported ZrB_2 or ZrB_2-SiC materials. Strength and toughness increased as the amount of SiC increased. Measured strengths ranged from ∼550 MPa for ZrB_2 to over 1000 MPa for ZrB_2-30% SiC. Likewise, toughness increased from 3.5 MPa to more than 5 MPa over the same composition range. The addition of SiC also improved oxidation resistance compared to pure ZrB_2.

Co-extrusion processing was used to produce ZrB_2-based ultra-high temperature ceramics with a fibrous monolithic structure. Samples had dense ZrB_2-30 vol% SiC cells approximately 100 μm in diameter surrounded by porous ZrB_2 cell boundaries approximately 20 μm thick. ZrB_2-based fibrous monoliths had four point bend strength of ∼450 MPa, about half of a conventional ZrB_2-SiC ceramic with the cell composition. Preliminary analysis of fracture behavior found that ZrB_2-based fibrous monoliths did not exhibit graceful failure because the difference in strength between the cell and cell boundary of the current materials was not sufficient.

1. Introduction

Transition metal borides and carbides such as ZrB_2, ZrC, HfB_2, HfC, and TaC have melting temperatures in excess of 3000°C making them candidates for use as structural materials at temperatures above 1800°C [1]. Within the family of ultra-high temperature ceramics (UHTCs), ZrB_2 has the lowest theoretical density (6.09 g/cm^3), which makes it attractive for aerospace applications [2]. Combined with its high melting temperature, ZrB_2 is reported to have excellent resistance to thermal shock and oxidation compared to other non-oxide structural ceramics [2]. In addition to aerospace applications, ZrB_2 has also been considered for use as electrode or crucible materials for molten metal contact [1–3]. Physical and mechanical property values reported in the recent technical literature for ZrB_2-based materials are summarized in Table I [1, 2, 4, 5].

ZrB_2-based ceramics can be prepared from commercial powders or synthesized using a variety of reaction-based methods [4–9]. Unintentional impurities [10] or processing additives [5, 9], which affect both the sintering behavior and high temperature performance, are often incorporated during processing. Additives or impurities can form low melting eutectics with UHTCs that have a deleterious effect on high temperature performance. As an example, the strength of ZrB_2 containing ∼3 volume percent Ni has been shown to drop by about 60% between 800°C and 1000°C [5]. Although a ZrB_2-Ni phase diagram has not been reported, the eutectic temperature is likely similar to that for the ZrC-Ni system, which was reported to be 1290°C [11]. Presumably, more refractory compounds would have less of an effect on high temperature performance. Reinforcement with SiC particulates has been shown to improve both the room temperature strength and oxidation resistance of ZrB_2 without sacrificing high temperature strength [12]. The first part of this study focused on the preparation, characterization, and testing of ZrB_2-SiC UHTCs prepared without oxide or low-melting temperature impurities.

Beyond the control of impurities and the addition of particulates, the thermo-mechanical performance of high temperature materials such as ZrB_2 can be tailored by manipulating the meso-scale (10–500 μm) structure. Co-extrusion of ceramic powder loaded thermoplastic polymers has been used to fabricate so-called fibrous monolithic structures with meso-scale architectures designed to improve thermo-mechanical performance [13, 14]. Using relatively inexpensive,

Corresponding author: Dr. Bill Fahrenholtz, Assistant Professor of Ceramic Engineering, 222 McNutt Hall, University of Missouri-Rolla, Rolla, MO 65409, USA.

TABLE I Reported room temperature bend strength, Young's Modulus, hardness, and fracture toughness values for ZrB_2-based ceramics

Composition	Strength (MPa)	Modulus (GPa)	Hardness (GPa)	Toughness ($MPa \cdot m_{1/2}$)	Reference
ZrB_2	480	490	21	3.7	[1]
ZrB_2	275–305	343–500	17.9–22	–	[2]
ZrB_2-20% SiC	506	–	21	4.0	[4]
ZrB_2-3% Ni	370	496	14.4	3.4	[5]

commercially available powders as precursors, multi-pass ram co-extrusion of core-shell type preforms has been used to fabricate ceramics that fail "gracefully" (i.e., provide some load retention after the initial failure event). The performance of fibrous monoliths is similar to the performance observed in continuous fiber ceramic composites produced from more expensive precursors using more complicated processing routes. Typical fibrous monolithic structures consist of a major phase (80–90 vol%) formed into strong, brittle "cells" that are surrounded by a thin (10–50 μm), continuous cell boundary phase (10–20 vol%) of a weaker material such as BN. By controlling structure on this scale, co-extrusion processing can be used to manipulate the fracture behavior of ceramics without changing the intrinsic properties of the material or significantly altering the composition of the component. For the second part of this study, ZrB_2-based fibrous monolithic structures were fabricated and characterized. The UHTC fibrous monoliths were made up of dense ZrB_2-SiC cells and porous ZrB_2 cell boundaries.

The purpose of this paper is to report the processing and characterization of ZrB_2-based UHTCs. Microstructure, mechanical properties, and oxidation behavior are reported for ZrB_2-SiC prepared by conventional hot pressing. In addition, the processing conditions and resulting microstructures of a novel ZrB_2-based fibrous monolithic ceramic are reported.

2. Experimental

2.1. Powder preparation for conventional ZrB_2 UHTCs

Conventional ZrB_2 and ZrB_2-SiC ultra-high temperature ceramics were prepared from commercial ZrB_2 (Grade B, H.C. Starck, Newton, MA, $\sim$2 μm) and SiC (UF-10, H.C. Starck, Newton, MA, $\sim$0.7μm). As-received powders were batched to produce ZrB_2 or ZrB_2 containing 10, 20, or 30 vol% SiC particulates. After batching, powders were attrition milled (Model HD-01, Union Process, Akron, OH) to reduce particle size and promote intimate mixing. A 750 ml polymer-lined bucket was charged with approximately 3000 g of WC media, 130 to 150 g of powder depending on the SiC content, and 250 ml of hexane. The mixture was milled for 2 h at 600 rpm using a polymer-coated spindle. Solvent was removed by rotary evaporation (Rotovapor R-124, Buchi, Flawil, Switzerland) to minimize segregation during drying.

2.2. Powder preparation and binder burnout for co-extrusion processing

ZrB_2-based fibrous monolithic ceramics were prepared by co-extrusion processing. Dense ZrB_2-SiC containing 30 vol% SiC was selected as the cell phase with porous ZrB_2 as the desired cell boundary phase. For the cell phase, ZrB_2 (Starck Grade B) and SiC (Starck UF-10) powders were attrition milled to reduce the average ZrB_2 particle size from $\sim$2 to $<$1 μm and uniformly disperse the SiC. Unmilled ZrB_2 (Grade A, H.C. Starck, Newton, MA, $\sim$6 μm) was used as the cell boundary phase. After the precursor powders and milling conditions were selected, separate binder formulations were developed for the cell and cell boundary materials using an iterative process. Precise data regarding the shear thinning behavior of the thermoplastic binder-powder mixtures were collected using a torque rheometer (C.W. Brabender, South Hackensack, NJ). Proper binder formulations are essential for development of the flow characteristics necessary to maintain the desired fibrous monolith architecture during the two-pass co-extrusion process. The behavior of the thermoplastics is generally shear thinning and can be described by an empirical power law relations similar to Equation 1 [15].

$$\tau = K\gamma^n \tag{1}$$

where τ is shear stress, K is the consistency index, γ is the shear rate, and n is the shear thinning exponent. The shear thinning exponent is a measure of the relative change in viscosity with shear rate [15]. If the viscosities of the cell and cell boundary batches are similar during batching and if the shear thinning exponent of the cell boundary is somewhat higher than the cell material, then mixing at the cell-cell boundary interface will be minimal as the preform is co-extruded. Basically, the lower viscosity material (cell boundary) will maintain its position at the periphery of the co-extrudate. In both the cell and the cell boundary phases, ethylene ethyl acrylate (EEA; DPDA-6182, Union Carbide, Danbury, CT) was used as the binder. For the cells, the binder was plasticized by adding methoxypolyethyleneglycol (MPEG-500; Union Carbide, Danbury, CT). For the cell boundaries, the binder was plasticized by addition of heavy mineral oil (HMO, Aldrich, Milwaukee, WI). The final binder amounts for the cell and cell boundary phases, along with the shear thinning exponents, are summarized in Table II.

Multi-core filaments were formed using a two pass co-extrusion process. The initial feedrod was

TABLE II Binder formulations and rheological constants for the cells and cell boundaries of ZrB_2-based fibrous monoliths

Component	Cell	Cell boundary
Composition	ZrB_2-30% SiC	ZrB_2
Binder	EEA	EEA
Binder content (vol%)	36	45
Plasticizer	Heavy mineral oil	MPEG-500
Plasticizer content (vol%)	7	4
Shear thinning exp.	0.30	0.54

approximately 2.5 cm in diameter and 10 cm long. Feedrods consisted of a fine particle size ZrB_2-30% SiC core and a coarse particle size ZrB_2 shell. Both the core and shell structures were prepared by mixing the powder and binder in a high shear mixer (C.W. Brabender, South Hackensack, NJ) above the softening temperature of the polymer. The UHTC fibrous monoliths were formed by extrusion at 0.6 mm/s, 110°C, and 39 MPa. The drawdown ratio was approximately 10:1 for all extrusion passes. After the first pass, the thin filaments were bound, pressed, and re-extruded to form the multi-core filament. After the second extrusion, the multi-core filaments were placed in a die and pressed (100°C, 10 MPa, 30 min) to form a rectangular plate (58 mm by 28 mm by 15 mm). The rectangular plate underwent binder burnout to prepare it for densification. The binder burnout cycle was 154 h long with a maximum temperature of 1054°C. The atmosphere during binder burnout was flowing air up to 280°C, followed by a change to argon.

2.3. Hot pressing conditions

Hot pressing was used to densify both conventional and fibrous monolithic UHTCs. Either milled ZrB_2-SiC powder mixtures or burned-out ZrB_2-SiC/ZrB_2 fibrous monolith preforms were placed in BN-coated, graphite foil-lined graphite dies. Samples were densified by hot pressing at 1900°C for 45 min at 32 MPa. The hot pressing atmosphere was argon.

2.4. Characterization and mechanical testing

After hot pressing, the bulk density of hot pressed billets was measured using the Archimedes' technique with water as the immersing medium. Helium pycnometry (1305 Multivolume, Micromeretics, Norcross, GA) was employed to estimate the true density of the hot pressed billets. For pycnometry, billets were ground to −325 mesh using a high purity alumina mortar and pestle to expose as much of the closed porosity as possible. The microstructure of the composites was examined using scanning electron microscopy (SEM; S570, Hitachi, Tokyo). Samples were prepared by cutting cross sections either parallel or perpendicular to the hot pressing direction. Chemical analysis was performed simultaneously with SEM using energy dispersive spectroscopy (EDS; AAT, X-ray Optics, Gainsville, FL). Vickers' hardness was determined from a minimum of ten indents that were formed using a load of 500 g and a dwell time of 30 s. The elastic constants were measured following the ASTM standard C1259-01 for impulse excitation of vibration. The fracture toughness was measured according to ASTM standard C1421, using a 30 kg load to form radial-median cracks followed by fracture in four-point bending. A minimum of seven bars were tested and averaged to obtain the value reported for each composition. Flexure strength was measured in four-point using a fully articulated test fixture according to ASTM standard C1161-02a for type A bars (25 mm × 2 mm × 1.5 mm). The reported values are the average of at least ten samples. Oxidation studies were conducted using thermal gravimetric analysis (TGA) following a proposed ASTM standard for oxidation testing [16]. The sample size was approximately 1 mm by 1.5 mm by 1.5 mm. Surface areas were calculated from external sample dimensions measured to ±0.01 mm. The weight changes for composites were measured under flowing air at a ramp rate of 10°C/min up to 1500°C without an isothermal hold. The resulting oxide layer was examined using SEM and EDS.

3. Results and discussion

3.1. Conventional ZrB_2-SiC UHTCs

Archimedes' density measurements for conventional ZrB_2-based UHTCs indicated that little or no porosity was present after hot pressing. With the exception of samples containing 10% SiC, the density of all of the samples was greater than 100% relative density based on the as-batched ZrB_2 and SiC contents (Table III) and the assumed theoretical densities of ZrB_2 (6.09 g/cm^3) and SiC (3.21 g/cm^3). The higher than predicted density of the hot pressed composites was attributed to the introduction of WC impurities during attrition milling. Comparison of bulk densities determined by the Archimedes' method to estimated true densities determined by helium pycnometry indicated that 1.4 to 2.2 vol% WC (theoretical density ∼15.0 g/cm^3 for WC bonded with 6% Co) was present in the hot pressed composites. The presence of WC was confirmed by XRD and SEM/EDS (discussed below). The low density of the 10% SiC sample (∼93% relative) manifests itself as large, isolated pores. Such pores might be formed by agglomeration of the starting powder or by an unknown chemical effect during hot pressing.

Examination of ZrB_2-SiC UHTCs by SEM showed that the SiC particles were well dispersed in the ZrB_2 matrix (Fig. 1). The SiC particle size ranged from less than a micron to approximately 5 μm. In addition to ZrB_2 and SiC, two other phases were observed. X-ray diffraction analysis (Fig. 2) and EDS confirmed the presence of WC (along with the possible presence of WC_{1-x} and/or W_2C) in the form of discrete particles (Fig. 1). An unidentified phase was observed by SEM. By EDS, it contained W, Zr and B. However, a reliable composition could not be determined by EDS nor could the low intensity, unindexed peaks in the XRD pattern

TABLE III Density of hot pressed ZrB_2-based UHTCs determined by Archimedes' method, calculated from ZrB_2 and SiC contents, and determined by He pycnometry along with the WC content of hot pressed composites

Composition	Archimedes' density (g/cm^3)	Theoretical density (g/cm^3)	Helium density (g/cm^3)	WC Content (vol%)
ZrB_2	6.26	6.09	6.27	1.9
ZrB_2-10% SiC	5.54	5.80	5.94	1.4
ZrB_2-20% SiC	5.69	5.51	5.74	2.3
ZrB_2-30% SiC	5.43	5.23	5.46	2.2

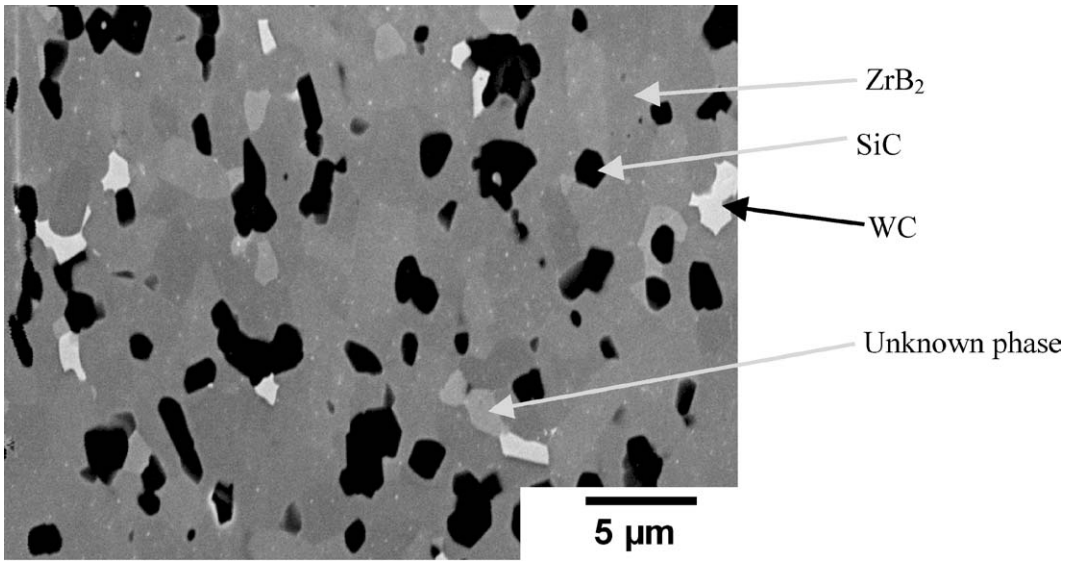

Figure 1 Polished cross section of a ZrB_2-20% SiC composite.

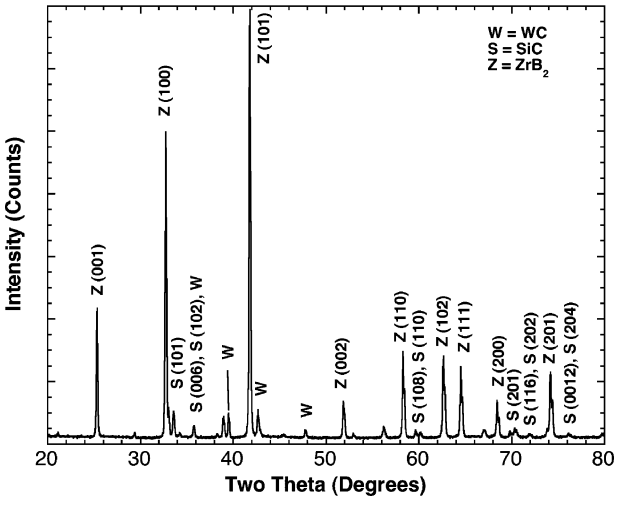

Figure 2 XRD pattern of ZrB_2-SiC composites after hot pressing, which indicated that ZrB_2 (Z), SiC (S), and WC or related phases (W) were present.

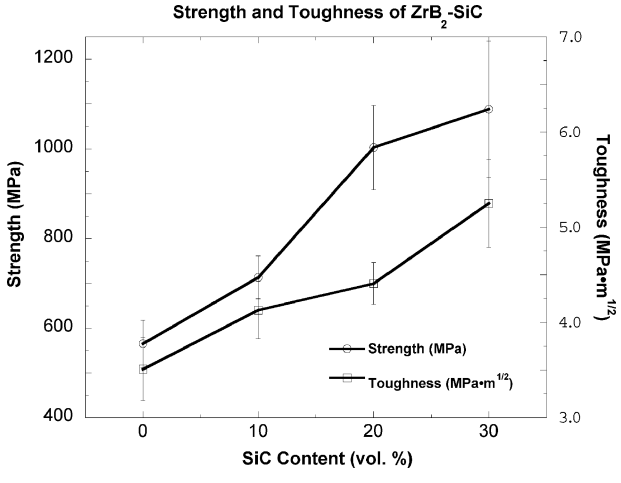

Figure 3 Four point bend strength and fracture toughness of ZrB_2-SiC as a function of SiC content.

be attributed to known Zr, B, C, Si, or W-containing phases. A previous investigation of phase equilibria in the Zr-B-W system postulated that a ternary phase might form, but the investigators could not confirm the composition or structure of the compound [17, 18]. A transmission electron microscopy study is underway in our laboratories to determine the composition and structure of this phase.

The hardness, Young's modulus, strength, and toughness were determined for ZrB_2-SiC as a function of SiC content. The modulus values were between 450 and 490 GPa (Table IV). A slight decrease in modulus was noted for the 10% SiC specimen, as would be expected for a porous material. Otherwise, no trend in modulus was observed as a function of composition. Likewise, no compositional trend was noted in hardness as all of the average values were ∼24 GPa (Table IV). Hardness was not adversely affected by the porosity of the 10% SiC sample, perhaps because none of the indents used to calculate the average value were in proximity to the relatively large, isolated pores. In contrast to modulus and hardness, the addition of SiC to ZrB_2 improved the bend strength and fracture toughness (Fig. 3). Pure ZrB_2 had an average strength of 565 MPa. Strength increased as SiC content increased to a maximum of 1089 MPa for the 30% SiC sample. The increase in strength has been attributed to a combination of grain size reduction and the WC impurities incorporated during milling [10]. Fracture toughness also increased as SiC content increased. For ZrB_2, a toughness of 3.5 MPa·$m_{1/2}$ was determined. Toughness increased to 5.3 MPa for the 30% SiC sample. To understand the toughening mechanism, the path of indentation cracks was examined in the SEM. As shown in Fig. 4, the SiC particles appear to bridge the cracks, which should

TABLE IV Hardness and modulus measured for ZrB_2-SiC

Composition	Hardness (GPa)	Modulus (GPa)
ZrB_2	23 ± 0.9	489
ZrB_2-10% SiC	24 ± 0.9	450
ZrB_2-20% SiC	24 ± 2.8	466
ZrB_2-30% SiC	24 ± 0.7	484

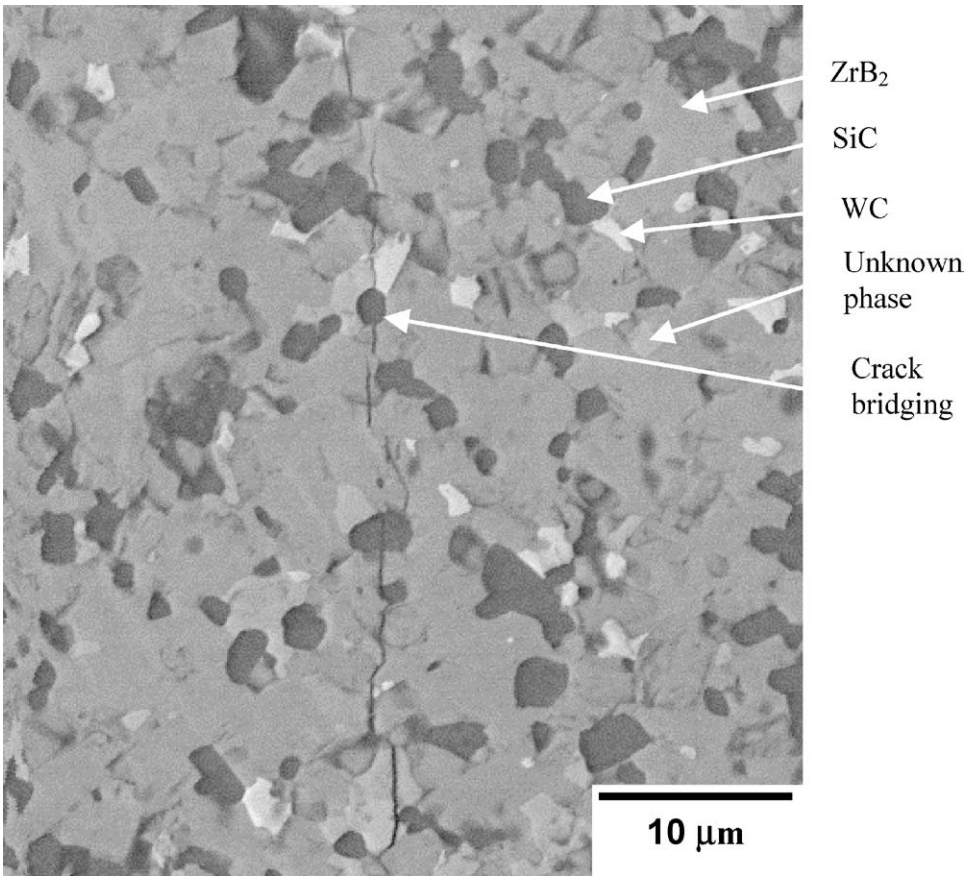

Figure 4 Path of an indentation crack in ZrB_2-20% SiC showing possible crack bridging.

increase toughness. The toughness increase observed for ZrB_2-SiC was nearly identical to the 2 MPa increase predicted by Ohji *et al*. for an analogous system (same relative elastic moduli and thermal expansion coefficients) that exhibited similar fracture behavior [19].

The addition of SiC to ZrB_2 also improved its oxidation resistance. Analysis by TGA found that weight gain began at ∼700°C when ZrB_2 or ZrB_2-SiC samples were heated in air. The rate of weight gain was similar for all compositions up to ∼1200°C. Above 1200°C, the oxidation rate of ZrB_2 increased dramatically resulting in a weight gain of 13.0 mg/cm^2 by 1500°C. The addition of SiC decreased the normalized weight gain (Table V) for ZrB_2 UHTCs; the sample containing 30% SiC gained the least weight at 1.8 mg/cm^2 by 1500°C. Examination by SEM/EDS showed that the higher oxidation resistance of the SiC-containing samples was imparted by a SiO_2-rich layer ∼4 μm thick that formed during heating (Fig. 5). No such layer was observed on ZrB_2 that did not contain SiC.

TABLE V Weight gain for ZrB_2-SiC as determined by TGA

Composition	Weight gain (mg/cm^2)
ZrB_2	13.0
ZrB_2-10% SiC	4.3
ZrB_2-20% SiC	3.1
ZrB_2-30% SiC	1.8

3.2. Co-extruded UHTCs

The bulk density of fibrous monoliths with ZrB_2-30% SiC cells and porous ZrB_2 cell boundaries was 5.11 g/cm^3 after hot pressing. Based on the helium pycnometry results on this composition, the relative density of the overall fibrous monolith was 91%. Assuming fully dense ZrB_2-30% SiC cells and a theoretical density of 6.1 g/cm^3 for the ZrB_2 cell boundaries, the relative density of the cell boundaries was estimated to be 72% using a rule of mixtures calculation. Examination of the microstructure by SEM revealed that the desired cellular architecture (high density ZrB_2-SiC cells with porous ZrB_2 grain boundaries) was maintained through the co-extrusion and densification steps (Fig. 6). Further, SEM analysis revealed that the cell boundaries were made up of grains that had an average size of nearly 10 μm with interconnected open porosity. The SiC inclusions were well distributed within the ZrB_2 matrix of the ZrB_2-SiC cells. Some closed porosity was observed in the cells, but the porosity was estimated to be less than 5 vol% and was not considered in the cell boundary density calculation. Some of porosity apparent on the polished surface has been attributed to grain pullout during polishing.

Analyses of hardness, modulus, and strength have been completed for ZrB_2-based fibrous monoliths (Table VI). The values were all less than the values measured for conventional ZrB_2-30% SiC that was used as the cell material. The bend strength of the fibrous monolith was ∼450 MPa, compared to ∼1000 MPa for the conventional UHTC with the same composition as

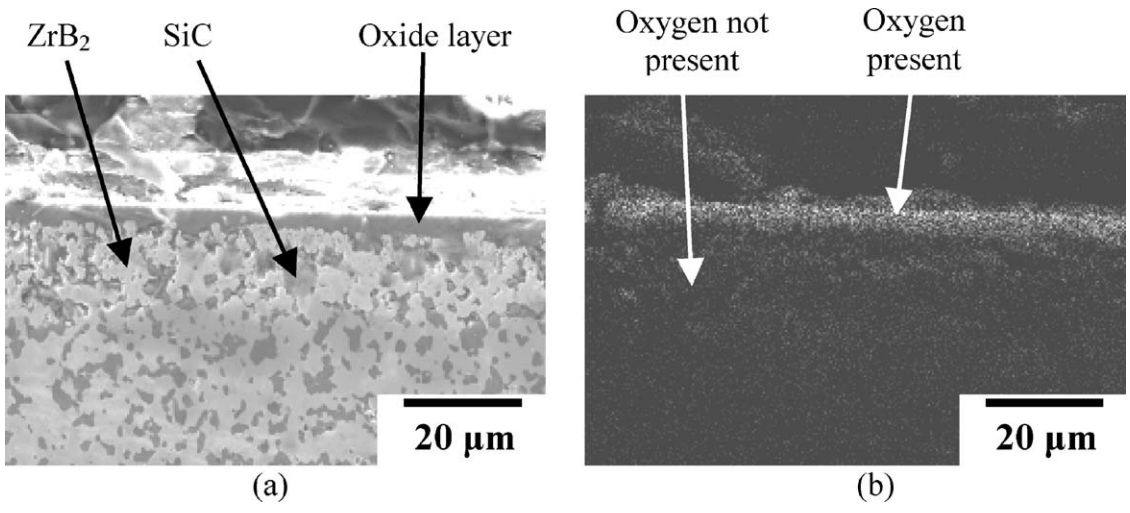

Figure 5 (a) An SEM image and (b) an oxygen map for ZrB_2-30% SiC after heating to 1500°C in air.

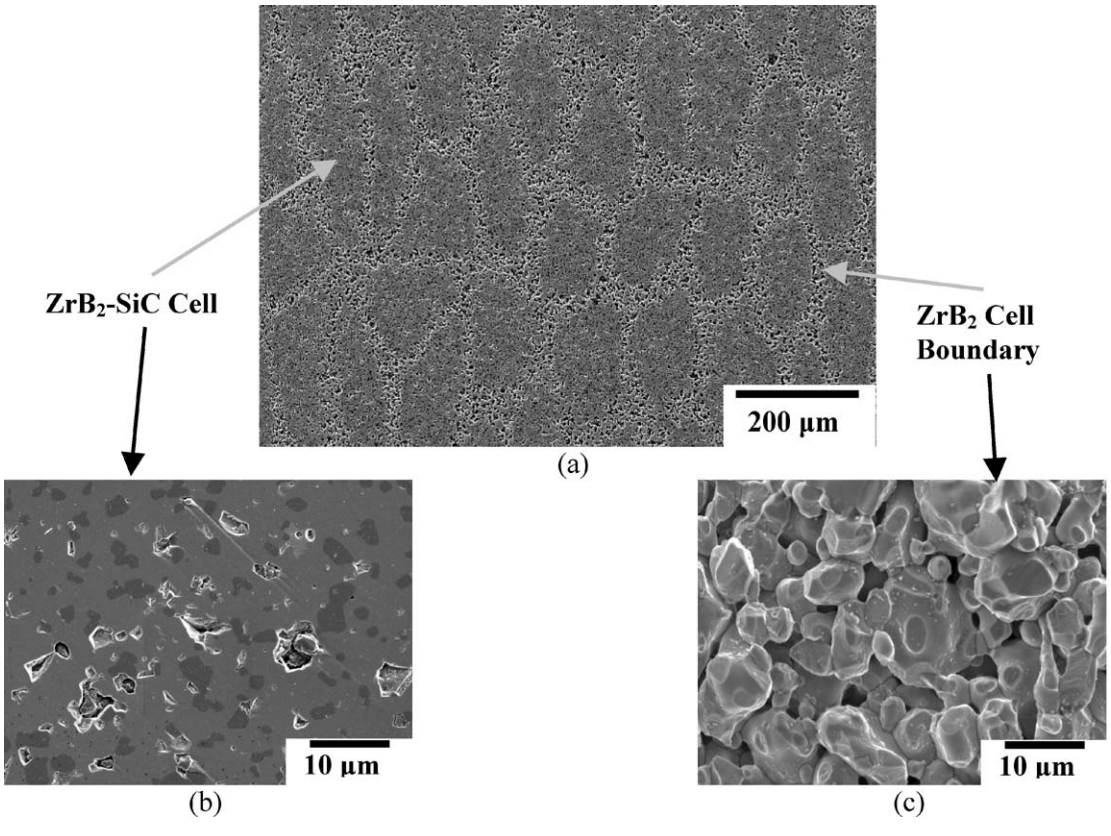

Figure 6 SEM micrographs of (a) a fibrous monolith with, (b) dense ZrB_2-SiC cells, and (c) porous ZrB_2 cell boundaries.

the cell phase. The measured elastic modulus of the fibrous monolith was 416 GPa. The measured modulus was nearly identical to a modulus of ~415 GPa that was predicted using a series mixing model. The mixing model assumed that the volume fraction of cell boundary phase was 0.3; it incorporated the measured modulus of the cell phase (484 GPa for ZrB_2-30% SiC from Table IV), and used a calculated modulus of the porous ZrB_2 cell boundary phase of 253 GPa. The modulus of the porous cell boundary phase was estimated using a relation for porous materials reported by Clegg, Equation 2 [20].

TABLE VI Average density, four-point bend strength, hardness, and modulus of ZrB_2-based fibrous monoliths compared to values for the cell and cell-boundary phases and a conventional ZrB_2-30% SiC ceramic

Composition	Density (g/cm^3)	Strength (MPa)	Hardness (GPa)	Modulus (GPa)
Fibrous monolith	5.11	459	–	416
ZrB_2-SiC cell	5.23	–	25	–
ZrB_2 cell boundary	4.00	–	7	–
ZrB_2-30% SiC	5.43	1031	24	484

$$E_P = E_o(1 - P)^2 \quad (2)$$

where E_P is the modulus of a porous ceramic, E_o is the modulus of a dense ceramic of the same composition, and P is the volume fraction porosity.

Based on the interaction of a fracture crack with the cellular architecture, the apparent fracture toughness of fibrous monolithic ceramics can increase by a factor of 10 or more compared to the measured fracture toughness of the cell material [14]. The fracture toughness of the cell material used in this fibrous monolith was 5.25 MPa·$m_{1/2}$ (Fig. 3). However, four point bend testing of ZrB_2-based fibrous monoliths found no indication of load retention after the initial fracture event, as has been observed in other fibrous monolith systems. Thus, only a minimal improvement in fracture toughness would be expected in these materials. Analysis of laminate structures by Clegg *et al*. suggests that a porosity level of ∼40% is necessary to sufficiently weaken a porous layer so that it can promote crack deflection [20], compared to less than 30% porosity in the porous cell boundaries in the fibrous monolith prepared in this study. Currently, specimen preparation and densification procedures are being modified to increase the porosity in the cell boundary to weaken it without adversely affecting the density of the cells. The first approach will be to evaluate the effect of using larger ZrB_2 particles for the cell boundaries. Larger particles should sinter less effectively, resulting in a lower relative density of the cell boundary. The second approach will be to add an inert polymeric filler to the cell boundary material (ZrB_2-thermoplastic polymer) prior to co-extrusion to decrease the solids loading of the cell boundary. The cell boundary porosity would be increased when the filler is removed during binder burnout.

4. Summary and conclusions

Conventional ZrB_2-based UHTCs were prepared by hot pressing. The addition of SiC improved mechanical performance and oxidation resistance of ZrB_2-based UHTCs. Four-point bend strength increased from ∼560 MPa for pure ZrB_2 to more than 1000 MPa for ZrB_2-30% SiC. Likewise, fracture toughness increased from ∼3.5 MPa·$m_{1/2}$ for pure ZrB_2 to more than 5 MPa·$m_{1/2}$ for ZrB_2-30% SiC. The increase in toughness was attributed to crack bridging by dispersed SiC particles in the ZrB_2 matrix. Oxidation behavior, examined using TGA, found that the weight gain decreased from 13.0 mg/cm^2 for pure ZrB_2 to 1.8 mg/cm^2 for ZrB_2-30% SiC. Improved oxidation resistance relative to pure ZrB_2 was imparted by the formation of a refractory SiO_2-based glassy layer on composites containing SiC.

ZrB_2-based fibrous monoliths were formed by co-extrusion processing. The fibrous monoliths had dense ZrB_2-30% SiC cells surrounded by porous ZrB_2 cell boundaries. From density measurements, the cell boundaries were ∼72% dense (∼28% porosity). The average strength of the ZrB_2-based fibrous monoliths was ∼450 MPa, compared to ∼1000 MPa for a conventional ZrB_2-30% SiC ceramic. Examination of the fracture behavior showed no load retention after the initial failure event in four point bend testing, indicating that further weakening of the grain boundary phase is needed to develop high apparent fracture toughness and promote graceful failure in ZrB_2-SiC/porous ZrB_2 fibrous monoliths.

Acknowledgements

This work was supported by the Ceramics and Non-Metallic Materials Program in the Air Force Office of Scientific Research on Grant Number F49620-03-1-0072. One of the authors, ALC, is supported by a Graduate Assistance in Areas of National Need (GAANN) Fellowship sponsored by the U.S. Department of Education and from a grant from the University of Missouri Research Board. The authors wish to thank Ms. Michelle Schaeffler for technical assistance. Finally, we would like to thank H.C. Starck for donating the Grade A ZrB_2 powder used in this work.

References

1. R. TELLE, L. S. SIGL and K. TAKAGI, in "Handbook of Ceramic Hard Materials" edited by R. Riedel (Wiley-VCH, Weinheim, 2000) p. 803.
2. R.A. CUTLER, in "Ceramics and Glasses, Engineered Materials Handbook", edited by S. J. Schneider, Jr. (ASM International, Materials Park, OH, 1991) p. 787.
3. N. KAJI, H. SHIKANO and I. TANAKA, *Taikabutsu Overseas* **44** (1992) 387.
4. G.-J. ZHANG, Z.-Y. DENG, N. KONDO, J.-F. YANG and T. OHJI, *J. Amer. Ceram. Soc*. **83** (2000) 2330.
5. F. MONTEVERDE, A. BELLOSI and S. BUICCIARDI, *J. Euro. Ceram. Soc*. **22** (2002) 279.
6. C. MROZ, "Zirconium Diboride", *Amer. Ceram. Soc. Bull*. **73** (1994) 141.
7. A. GOLDSTEIN, Y. GEFFEN and A. GOLDENBERG, *J. Amer. Ceram. Soc*. **84** (2001) 642.
8. H. ZHAO, Y. HE and Z. JIN, *ibid*. **78** (1995) 2534.
9. S. K. MISHRA, S. K. DAS, A. K. RAY and P. RAMACHANDRARAO, *ibid*. **85** (2002) 2846.
10. A. L. CHAMBERLAIN, W. G. FAHRENHOLTZ, G. E. HILMAS and D. T. ELLERBY, "High Strength ZrB_2-Based Ceramics," *J. Amer. Ceram. Soc*. **87**(6) (2004) 1170.
11. Figure 9020 in "Phase Equilibria Diagrams—Phase Diagrams for Ceramists Vol. X: Borides, Carbides, and Nitrides", edited by A. E. McHale (The American Ceramic Society, 1994).
12. E. CLOUGHERTY, R. HILL, W. RHODES and E. PETERS, "Research and Development of Refractory Oxidation-Resistant Diborides, Part II, Vol. II: Processing and Characterization", Technical Report No. AFML-TR-68-190 (1970).
13. D. POPOVICH, J. W. HALLORAN, G. E. HILMAS, G. A. BRADY, G. ZYWICKI, S. SOMERS and A. BARDA, "Process for Preparing Textured Ceramic Composites", U.S. Patent No. 5,645,781, issue date July 8, 1997.
14. G. E. HILMAS, G. A. BRADY and J. W. HALLORAN, in Ceramic Transactions, Vol. 51, Fifth Int'l Conf. on Ceramic Processing Science and Technology, edited by H. Hausner, G. L Messing and S.-I. Hirano (American Ceramic Society, Westerville, OH, 1995) p. 609.
15. J. S. REED, in "Principles of Ceramics Processing" (John Wiley and Sons, New York, 1995) p. 280.
16. "High Temperature Oxidation Exposure Testing of Non-Oxide Advanced Ceramics at Atmospheric Pressure and Low Gas Velocities", under consideration by ASTM C-28.
17. Figure 8851 in "Phase Equilibria Diagrams—Phase Diagrams for Ceramists Vol. X: Borides, Carbides, and Nitrides", edited by A. E. McHALE (The American Ceramic Society, 1994).
18. E. RUDY, "Part V. Compendium of Phase Diagram Data", Ternary Phase Equilibria in Transition Metal-Boron-Carbon-Silicon Systems, Technical Report AFML-TR-65-2, Air Force Materials Laboratory, Wright-Patterson Air Force Base, OH (1969).
19. T. OHJI, Y. K. JEONG, Y. H. CHOA and K. NIIHARA, *J. Amer. Ceram. Soc.* **81** (1998) 1453.
20. K. S. BLANKS, A. KRISTOFFERSSON, E. CARLSTÖM and W. J. CLEGG, *J. Euro. Ceram. Soc.* **18** (1998) 1945.

Received 9 October 2003
and accepted 15 March 2004